ELSEVIER

Journal of Chromatography A, 775 (1997) 211–224

JOURNAL OF CHROMATOGRAPHY A

Deposition parameters of air pollutants on solid surfaces, measured in the presence of surface and gaseous reactions, with a simultaneous determination of the experimental isotherms

Ch. Abatzoglou[a], E. Iliopoulou[a], N.A. Katsanos[a,*], F. Roubani-Kalantzopoulou[b], A. Kalantzopoulos[b]

[a]*Physical Chemistry Laboratory, University of Patras, 26500 Patras, Greece*
[b]*Department of Chemical Engineering, National Technical University, 15780 Zografou, Athens, Greece*

Received 31 December 1996; revised 27 February 1997; accepted 28 February 1997

Abstract

A method is described for measuring deposition velocities and reaction probabilities of air pollutants with solid surfaces, in the presence of a chemical reaction between two pollutants in the gas phase above the solid. The theoretical analysis is based on experimental adsorption isotherms measured simultaneously through the local adsorption parameters, together with the rate constants for desorption, first-order surface reaction and gaseous chemical reactions. The experimental procedure is that of the reversed-flow gas chromatography (RF-GC) technique, the analysis of the diffusion bands being effected by a personal computer programme. The methodology has been applied to the action of gaseous hydrocarbons on two metal oxides, and of dimethyl sulfide on Penteli marble particles and on pieces obtained from three archaeological statues. All physicochemical parameters mentioned above were measured both in the absence and in the presence of a second gaseous pollutant (NO_2). The synergistic effects in the gas phase on the various deposition parameters was fairly obvious. © 1997 Elsevier Science B.V.

Keywords: Deposition velocity; Reaction probability; Adsorption isotherms; Synergistic effect; Hydrocarbons, gaseous; Metal oxides; Dimethyl sulfide

1. Introduction

The use of denuder tubes with gas chromatographic (GC) instrumentation was recently described [1] as a means to measure deposition velocities and reaction probabilities of air pollutants with solid surfaces, in the presence of a chemical reaction between two pollutants in the gas phase above the solid. Although this places synergistic effects of air pollutants on a quantitative scientific basis, the description was only part of a review [1] and therefore short. Moreover, the mathematical modelling and the solution of the system of partial differential equations was based on a linear adsorption isotherm of the pollutant analytes.

In a more recent paper [2], however, a simple determination of experimental isotherms, using the same experimental arrangement as above, was introduced leading directly to independent isotherms over a wide range of pollutant concentrations, without specifying a priori an isotherm equation. Combining the two above situations and using a solid bed

*Corresponding author.

0021-9673/97/$17.00
PII S0021-9673(97)00232-X

analogous with that of catalytic studies, a method is developed here which permits the simultaneous determination of the following physicochemical parameters under non-steady-state conditions: (1) The dynamic adsorption rate constant k_1 of the analyte pollutant A, describing its local experimental isotherm on the surface of the solid varying with time; (2) the desorption rate constant of A from the solid surface k_{-1}; (3) the rate constant k_2 of a possible first- or pseudofirst-order surface reaction of the adsorbed analyte A leading to the final damage of the solid; (4) the apparent first-order rate constant k_{app} of a chemical reaction of A with another pollutant B in the gaseous phase above the solid, pertaining to synergistic effects; (5) the overall deposition velocity V_d and reaction probability γ of A on the solid, under the influence of the gaseous reaction and the real adsorption isotherm. This is equivalent to an overall mass transfer coefficient of the gaseous pollutant to the solid material, corrected for activated adsorption–desorption and surface reactions.

The achievement described above can also be used most effectively in kinetics of heterogeneous catalysis on surfaces, measuring simultaneously the homogeneous gas phase rate constant of the reaction A+B→products, taking into account the real experimental adsorption isotherm of A. The Langmuir, BET or other isotherm is not necessary to be assumed a priori.

2. Theoretical analysis

2.1. The mathematical model

The relations used for calculating the physicochemical parameters described in points (1) to (5) in Section 1 are derived below by reference to Fig. 1, which is practically the same as that used in a recent catalytic study [3]. The length coordinate along the diffusion column is artificially divided into the z and y sections, to make the mathematical description much easier. Otherwise, Heaviside unit step functions will be necessary to separate the physical phenomena in the catalyst bed from those in the diffusion column. These functions will complicate the solution of the partial differential equations by double Laplace transforms.

An amount m (mol) of the pollutant analyte A can be injected instantaneously as a small volume pulse (delta function), either at $z=L_1$ or at $y=L_2$:

$$c_z(0,z) = \frac{m}{a_z}\delta(z - L_1) \quad (1)$$

$$c_y(0,y) = \frac{m}{a_y}\delta(y - L_2) \quad (2)$$

where $c_z(0, z)$=initial ($t=0$) gaseous concentration (mol/cm^3) of pollutant A along the axial coordinate z (cm) of the diffusion column; $c_y(0,y)$=initial

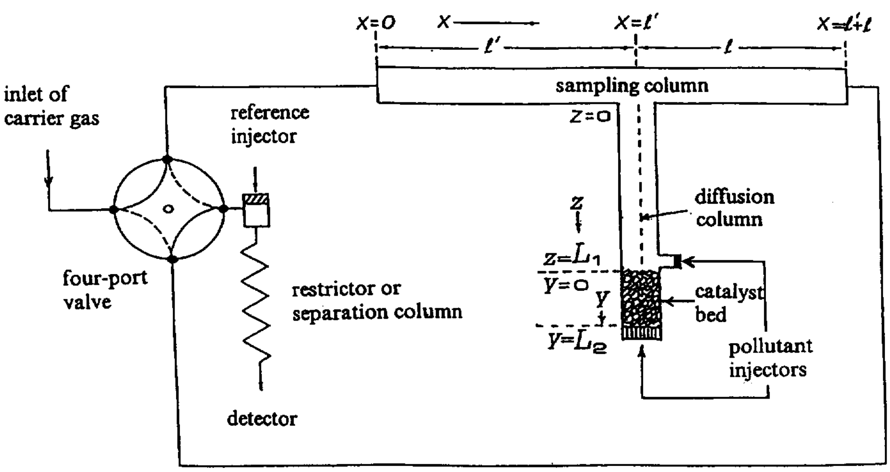

Fig. 1. Outline of the experimental arrangement used in catalysis studies [3], as modified for injection at $z=L_1$.

gaseous concentration (mol/cm^3) of A along the length coordinate y (cm) of the solid bed and a_z, a_y = cross sectional areas (cm^2) of the void spaces in regions z and y, respectively.

The following mathematical analysis is based on the initial condition (Eq. (2)), i.e., solute injection at $y = L_2$.

The mass balance equations in both regions y and z are approximately taken in one dimension, since the column radii used experimentally were much smaller than column lengths.

2.1.1. Region y

In this region of the cell (cf. Fig. 1) the mass balance equation for the gaseous concentration of A, $c_y = c_y(t, y)$, with respect to time t is

$$\frac{\partial c_y}{\partial_t} = D_2 \frac{\partial^2 c_y}{\partial y^2} - k_{-1} \frac{a_s}{a_y}(c_s^* - c_s) - k_{app} c_y \quad (3)$$

where D_2 = diffusion coefficient into the carrier gas of analyte A in section y (cm^2/s); a_s = amount of solid material per unit length of column bed (g/cm); c_s = concentration of A adsorbed on the solid at time t (mol/g); c_s^* = equilibrium adsorbed concentration of A at time t (mol/g); k_{-1} = rate constant for desorption from the bulk solid (s^{-1}) and k_{app} = apparent first-order rate constant for the gaseous reaction of A with another pollutant B in the void space of section y above the solid (s^{-1}).

The rate of change of the adsorbed concentration c_s is described [4] by the relation

$$\frac{\partial c_s}{\partial t} = k_{-1}(c_s^* - c_s) - k_2 c_s \quad (4)$$

where k_2 is the rate constant (s^{-1}) of a possible first-order or pseudofirst-order surface reaction of the adsorbed pollutant.

Taking the Laplace transforms of the terms of Eqs. (3) and (4) with respect to time t, under the initial condition (Eq. (2)) for c_y and $c_s(0, y) = 0$ for c_s, and then eliminating the transformed function c_s between the two transformed equations, one obtains

$$\frac{d^2 C_y}{dy^2} = -\frac{m}{a_y D_2}\delta(y - L_2) + \frac{p + k_{app}}{D_2} C_y + \frac{k_{-1} a_s}{D_2 a_y} \times \frac{p + k_2}{p + k_{-1} + k_2} C_s^* \quad (5)$$

where the capital letters C_y and C_s^* denote the transformed functions c_y and c_s^*, respectively, and p the transform parameter.

The relation between c_y and c_s^* is described by the local adsorption isotherm

$$c_s^* = \frac{m_s}{a_s}\delta(y - L_2) + \frac{a_y}{a_s} k_1 \int_0^t c_y(\tau) d\tau \quad (6)$$

where m_s is the amount of analyte A (mol) which would be adsorbed at equilibrium initially, τ is a dummy variable for time, and k_1 the local adsorption parameter (s^{-1}), transforming the area under the c_y vs. t curve into c_s^*. As mentioned in Section 1, this relation describes the actual experimental isotherm, not necessarily a linear one, without the help of an a priori isotherm equation (Langmuir, BET, etc.). The graphical experimental isotherm can be constructed in detail if one desires [2], but in the present work this is not necessary. Only the basic definition (Eq. (6)) suffices to incorporate the exact isotherm into the mathematical calculations. The non-linearity in general is automatically taken into account.

The Laplace transformation with respect to time of the terms of Eq. (6) gives

$$C_s^* = \frac{m_s}{a_s} \cdot \frac{\delta(y - L_2)}{p} + \frac{a_y k_1 C_y}{a_s p} \quad (7)$$

and this is substituted for C_s^* in Eq. (5). The result is a second-order differential equation of C_y with respect to the length coordinate y:

$$\frac{d^2 C_y}{dy^2} - q_2^2 C_y = -P\delta(y - L_2) \quad (8)$$

where

$$q_2^2 = \frac{1}{D_2}\left[p + k_{app} + \frac{k_1 k_{-1}(p + k_2)}{p(p + k_{-1} + k_2)} \right] \quad (9)$$

and

$$P = \frac{1}{D_2 a_y}\left[m - \frac{m_s k_{-1}(p + k_2)}{p(p + k_{-1} + k_2)} \right] \quad (10)$$

Eq. (8) can be solved by taking further Laplace transforms with respect to y of all terms, rearranging and inversing the y transforms. The result is

$$C_y = C_y(0)\cosh q_2 y + \frac{C'_y(0)}{q_2}\sinh q_2 y - \frac{P}{q_2}\sinh q_2(y - L_2)\cdot u(y - L_2) \quad (11)$$

where $C_y(0)$ is the t transform of c_y at $y=0$, $C'(0)=(\mathrm{d}C_y/\mathrm{d}y)_{y=0}$, and $u(y-L_2)$ is the unit step function.

The boundary values $C_y(0)$ and $C'_y(0)$ are not known, but at the other boundary of the y region, $y=L_2$, $(\partial c_y/\partial y)_{y=L_2}=0$, since there is no flux across this boundary. The t Laplace transform of this boundary condition is simply $(\mathrm{d}C_y/\mathrm{d}y)_{y=L_2}=0$, and if this is used with Eq. (11), it gives after rearrangement

$$C'_y(0) = \frac{P}{\cosh q_2L_2} - C_y(0)q_2\tanh q_2L_2 \quad (12)$$

2.1.2. Region z

This region is empty of any solid material (cf. Fig. 1) and the mass balance equation for the pollutant A, in the presence of a first-order or pseudofirst-order chemical reaction in the gaseous phase, is

$$\frac{\partial c_z}{\partial t} = D_1\frac{\partial^2 c_z}{\partial z^2} - k_{\mathrm{app}}c_z \quad (13)$$

where $c_z=c_z(t, z)$ is the gaseous concentration of A (mol/cm^3), and the apparent rate constant k_{app} is assumed the same as that in the gaseous region y, if both regions z and y are kept at the same temperature. The same applies to the gaseous diffusion coefficient D_1 of A into the carrier gas in region z as compared to that in the empty region y.

As was done before [5] for an equation like Eq. (13) without the last term, taking double Laplace transforms with respect to t and initial condition $c_z(0, z)=0$, and then with respect to z, one finds after inversion of the latter

$$C_z = C_z(0)\cosh q_1z + \frac{C'_z(0)}{q_1}\sinh q_1z \quad (14)$$

where capital letters like C_z indicate t transformed concentrations, as before, $C_z(0)$ refers to $z=0$ and $C'_z(0)=(\mathrm{d}C_z/\mathrm{d}z)_{z=0}$. The q_1 is given by the relation

$$q_1^2 = \frac{p + k_{\mathrm{app}}}{D_1} \quad (15)$$

Denoting by $c(l',t)$ the concentration of the analyte A in the sampling column of Fig. 1, at time t and $x=l'$, and $C(l', p)$ its t Laplace transform, the boundary conditions at $z=0$ are formulated as

$$c_z(0) = c(l', t) \text{ and } D_1\left(\frac{\partial c_z}{\partial t}\right)_{z=0} = vc(l', t) \quad (16)$$

where v (cm/s) is the mean linear velocity of the carrier gas in the sampling column. Using the t transforms of these conditions in Eq. (14), it becomes

$$C_z = C(l', p)\left[\cosh q_1z + \frac{v}{D_1q_1}\sinh q_1z\right] \quad (17)$$

2.1.3. Linking the solutions in regions z and y

This is done with the help of the boundary conditions at $z=L_1$ and $y=0$:

$$C_y(0) = C_z(L_1) \quad (18)$$

$$a_yD_2\left(\frac{\mathrm{d}C_y}{\mathrm{d}y}\right)_{y=0} = a_zD_1\left(\frac{\mathrm{d}C_z}{\mathrm{d}z}\right)_{z=L_1} \quad (19)$$

From Eq. (17) both $C_z(L_1)$ and $(\mathrm{d}C_z/\mathrm{d}z)_{z=L_1}$ are calculated. After omission of the term $\cosh q_1L_1$ compared with $(v/D_1q_1)\sinh q_1L_1$, and of the term $\sinh q_1L_1$ compared with $(v/D_1q_1)\cosh q_1L_1$, as was done before [6,7], and substitution into Eqs. (18) and (19), $C_y(0)$ and $(\mathrm{d}C_y/\mathrm{d}y)_{y=0}=C'_y(0)$ are found. These then are substituted for $C_y(0)$ and $C'_y(0)$, respectively, in Eq. (12) with the result, after algebraic manipulations and rearrangements,

$$C(l', p) = \frac{A}{\dot{V}}\cdot\frac{m - m_sq_3}{A\cosh q_1L_1\cdot\cosh q_2L_2 + J\sinh q_1L_1\cdot\sinh q_2L_2} \quad (20)$$

where $\dot{V}=azv$ is the volumetric flow-rate of the carrier gas, and

$$A = \frac{a_z}{a_y}, \quad J = \frac{D_2q_2}{D_1q_1} \quad (21)$$

q_1 being given by Eq. (15), q_2 by Eq. (9), and q_3 by the relation

$$q_3 = \frac{k_{-1}(p + k_2)}{p(p + k_{-1} + k_2)} \quad (22)$$

The rest of the symbols in Eqs. (20)–(22) have been defined before.

Now, we expand both $\cosh qL$ and $\sinh qL$ in the denominator of Eq. (20) in McLaurin series in qL, retaining only the first two terms, i.e., cosh $qL=1+q^2L^2/2$, and sinh $qL=0+qL=qL$. Then, one substitutes Eqs. (15) and (9) and Eq. (22) for q_1, q_2 and q_3, respectively, to find (leaving out extended mathematical details)

$$C(l', p) = \frac{m\alpha_1\alpha_2}{\dot{V}} \cdot \frac{p^2 + [k_{-1}(1 - m_s/m) + k_2]p - m_s k_{-1} k_2/m}{p^4 + Xp^3 + Yp^2 + Zp + W} = \frac{m\alpha_1\alpha_2}{\dot{V}} \cdot \frac{p^2 + [k_{-1}(1 - m_s/m) + k_2]p - m_s k_{-1} k_2/m}{(p - B_1)(p - B_2)(p - B_3)(p - B_4)} \quad (23)$$

In these equations

$$\alpha_1 = \frac{2D_1}{L_1^2}, \quad \alpha_2 = \frac{2D_2}{L_2^2} \quad (24)$$

whilst B_1, B_2, B_3 and B_4 are the roots of the polynomial in the denominator, related to the coefficients X, Y, Z and W and the physicochemical parameters k_1, k_{-1}, k_2 and k_{app} through the equations

$$X = \alpha_2(1 + V_1) + 2k_{app} + k_{-1} + k_2 = -(B_1 + B_2 + B_3 + B_4) \quad (25)$$

$$Y = [\alpha_2(1 + V_1) + 2k_{app}](k_{-1} + k_2) + \alpha_1\alpha_2 + k_1k_{-1} + k_{app}^2 + \alpha_2(1 + V_1)k_{app} = B_1B_2 + B_1B_3 + B_1B_4 + B_2B_3 + B_2B_4 + B_3B_4 \quad (26)$$

$$Z = \alpha_1\alpha_2(k_{-1} + k_2) + \alpha_2V_1k_1k_{-1} + k_1k_{-1}k_2 + \alpha_2(1 + V_1)(k_{-1} + k_2)k_{app} + k_1k_{-1}k_{app} + k_{app}^2(k_{-1} + k_2) = -(B_1B_2B_3 + B_1B_2B_4 + B_1B_3B_4 + B_2B_3B_4) \quad (27)$$

$$W = (\alpha_2V_1 + k_{app})k_1k_{-1}k_2 = B_1B_2B_3B_4 \quad (28)$$

The volume ratio V_1 is given by the relation

$$V_1 = \frac{2V'_G(\text{empty})\epsilon}{V_G} + \frac{\alpha_1}{\alpha_2} \quad (29)$$

where V_G and V'_G are the gaseous volumes of empty sections L_1 and L_2, respectively, (cf. Fig. 1) and ϵ the external porosity of the solid bed.

Taking into account that the height H of the extra chromatographic peaks, obtained by the repeated flow reversals, is proportional to the concentration $c(l', t)$, $H^{1/M} = gc(l', t)$, M being the response factor of the detector and g the proportionality constant, determined as described elsewhere [2], we write the result of the inverse Laplace transforms with respect to p of Eq. (23) as

$$H^{1/M} = gc(l', t) = A_1\exp(B_1t) + A_2\exp(B_2t) + A_3\exp(B_3t) + A_4\exp(B_4t) \quad (30)$$

where the exponential coefficients of time B_1, B_2, B_3 and B_4 satisfy Eqs. (25)–(28), while the pre-exponential factors A_1, A_2, A_3 and A_4 are explicit functions of $gm\alpha_1\alpha_2/\dot{V}$ of B_1, B_2, B_3, B_4, k_{-1}, k_2, m and m_s. The analytical form of these is not needed.

All the above theoretical analysis has been based on the initial condition described by Eq. (2), i.e., on an injection of the analyte at the point $y = L_2$. If the injection, again as an instantaneous pulse, were made at $z = L_1$ (*cf.* Fig. 1), the initial condition would be given by Eq. (1), and the mathematical analysis would lead again to Eqs. (24)–(30), with the only difference being the analytical functions defining A_1, A_2, A_3 and A_4 which now are not functions of m_s. Again the detailed form of these functions is not needed.

2.2. Determination of k_{app}

In order that the values of k_1, k_{-1} and k_2 are extracted from the experimental H and t values, through Eqs. (24)–(30), an independent path for calculating k_{app} is needed. This is effected by assuming a steady-state for c_s in Eq. (4), $dc_s/dt = 0$, leading to

$$k_{-1}(c_s^* - c_s) - k_2c_s = 0 \quad (31)$$

Using this in place of Eq. (4), Eq. (5) becomes

$$\frac{d^2C_y}{dy^2} = -\frac{m}{a_yD_2}\delta(y - L_2) + \frac{p + k_{app}}{D_2}C_y + \frac{k_{-1}a_s}{D_2a_y} \times \frac{k_2}{k_{-1} + k_2}C_s^* \quad (32)$$

Substituting Eq. (7) for C_s^* as before, an equation analogous to Eq. (8) is obtained. Following exactly the same route as before, one reaches the relation

$$C(l', p) = \frac{m\alpha_1\alpha_2}{\dot{V}} \cdot \frac{p - F}{p^3 + X_1 p^2 + Y_1 p + Z_1} = \frac{m\alpha_1\alpha_2}{\dot{V}} \cdot \frac{p - F}{(p - B_5)(p - B_6)(p - B_7)} \quad (33)$$

where α_1, α_2 and V_1 are given by Eqs. (24) and (29),

$$F = \frac{m_s}{m} \cdot \frac{k_{-1}k_2}{k_{-1} + k_2} \quad (34)$$

$$X_1 = \alpha_2(1 + V_1) + 2k_{app} = -(B_5 + B_6 + B_7) \quad (35)$$

$$Y_1 = \alpha_1\alpha_2 + \frac{k_1k_{-1}k_2}{k_{-1} + k_2} + \alpha_2(1 + V_1)k_{app} + k_{app}^2 = B_5B_6 + B_5B_7 + B_6B_7 \quad (36)$$

$$Z_1 = \frac{(\alpha_2V_1 + k_{app})k_1k_{-1}k_2}{k_{-1} + k_2} = -(B_5B_6B_7) \quad (37)$$

and B_5, B_6 and B_7 are the roots for p of the denominator in Eq. (33). Eq. (33) is similar to Eq. (23), and its inverse Laplace transforms with respect to p gives a function of time analogous to Eq. (30):

$$H^{1/M} = gc(l', t) = A_5\exp(B_5t) + A_6\exp(B_6t) + A_7\exp(B_7t) \quad (38)$$

where A_5, A_6 and A_7 are given by expressions independent of time, as A_1, A_2, A_3 and A_4 of Eq. (30).

2.3. Calculations

Using non-linear regression analysis PC programs in GW-BASIC, one can calculate the exponential coefficients of time B_1, B_2, B_3 and B_4 of Eq. (30), as well as the coefficients B_5, B_6 and B_7 of Eq. (38), from the experimental pairs of values H, t, where H is the height (in arbitrary units, say cm) of the sample chromatographic peaks and t the respective times, when flow-reversal of the carrier gas was made. These programs have been based on a fortran IV computer program of Sedman and Wagner [11], dealing with polyexponential parameter estimates. As one can see from the Appendix here (cf. lines 20 and 30) the present program is not a single seven exponential function for extracting B_1, B_2,..., B_7 from the experimental H, t values, but two functions, one with four exponentials and the other with three exponentials. The exponential stripping method is guided by the overall goodness of fit expressed by the square of correlation coefficient r^2. This universally accepted criterion is calculated according to Eq. 5 of Ref. [11] (cf. lines 1030 and 1820 of Appendix). The maximum values of r^2 for the four and three exponential functions finally selected are printed in the lines 1250 and 1970, respectively. These are given as r_4^2, r_3^2 in the last column of Tables 1 and 2. It is seen that in most cases they are in the range 0.991–0.999, showing a remarkable goodness of fit for a non-linear regression analysis. The "t" test of significance for the smallest r^2 found, shows that it is highly significant, with a probability to be exceeded smaller than 0.05%. The program also prints, together with the B values, their standard errors (cf. lines 1140, 1170, 1200, 1230, 1910, 1930 and 1950 for B_1, B_2, B_3, B_4, B_5, B_6 and B_7, respectively). The errors found in all runs are reasonable for physicochemical measurements. Analogous PC programs have already been published [1,2,5].

From the values of B_1, B_2, B_3, B_4, B_5, B_6 and B_7, one calculates the auxiliary coefficients X, Y, Z, W, X_1, Y_1 and Z_1 by using Eqs. (25)–(28), (35)–(37). From these in turn, the calculation of k_1, k_{-1}, k_2 and k_{app} is carried out as follows: The sum $k_{-1}+k_2$ is obtained from the difference $X-X_1$, from the ratio W/Z_1, or as a mean value of these two. Subtraction of $k_{-1}+k_2$ from X gives the value of $\alpha_2(1+V_1)+2k_{app}$. Then, using the value of $\alpha_2(1+V_1)$ found before by conducting the same experiment in the absence of the second analyte B, k_{app} is calculated. Also from $\alpha_2(1+V_1)$, α_2V_1 is easily computed since V_1 is known from the geometrical characteristics of the cell. The calculation of k_1k_{-1} follows from the relation

$$k_1k_{-1} = \left\{ Y - [\alpha_2(1 + V_1) + 2k_{app}](k_{-1} + k_2) - \frac{Z}{k_{-1} + k_2} + \frac{W}{(\alpha_2V_1 + k_{app})(k_{-1} + k_2)} \right\} \Big/ \left(1 - \frac{\alpha_2V_1 + k_{app}}{k_{-1} + k_2}\right) \quad (39)$$

Then, dividing W by $\alpha_2V_1+k_{app}$ and by k_1k_{-1} gives the value of k_2. The value of k_{-1} follows from the difference $(k_{-1}+k_2)-k_2$, and that of k_1 from the ratio k_1k_{-1}/k_{-1}. The α_1 is calculated either from Eq. (26) or from Eq. (27).

The deposition velocity V_d is given by the relation

Table 1

Local adsorption parameters (k_1), desorption rate constants (k_{-1}), surface reaction rate constants (k_2), deposition velocites (V_d), reaction probabilities (γ) and apparent gaseous reaction rate constants (k_{app}) of gaseous hydrocarbons A ($3.2 \cdot 10^{-3}$ mol/dm^3), interacting with the surface of two solids S (Cr_2O_3 and ZnO), in the absence and in the presence of another gas B (NO_2, $6.5 \cdot 10^{-4}$ mol/dm^3), at 323.2 K

A/S/B	k_1 (10^{-4} s^{-1})	k_{-1} (10^{-3} s^{-1})	k_2 (10^{-5} s^{-1})	V_d (10^{-10} cm s^{-1})	γ (10^{-14})	k_{app} (10^{-4} s^{-1})	r_4^2, r_3^2
C_2H_2/Cr_2O_3[a]	15.5	9.99	3.83	1.32	1.51	–	0.999, 0.996
$C_2H_2/Cr_2O_3/NO_2$	15.3	8.15	3.07	1.29	1.48	1.95	0.999, 0.995
C_2H_4/Cr_2O_3[a]	14.2	16.7	3.85	0.733	0.839	–	0.999, 0.996
$C_2H_4/Cr_2O_3/NO_2$	1.03	0.374	231	27.5	31.5	6.03	0.992, 0.990
C_2H_6/Cr_2O_3[a]	9.40	8.15	4.29	1.10	1.26	–	0.998, 0.997
$C_2H_6/Cr_2O_3/NO_2$	3.03	0.430	13.4	16.2	18.5	6.11	0.998, 0.998
C_3H_6/Cr_2O_3[a]	9.02	6.25	1.33	0.428	0.490	–	0.998, 0.995
$C_3H_6/Cr_2O_3/NO_2$	9.46	10.3	3.56	0.726	0.831	0.646	0.997, 0.992
1-C_4H_8/Cr_2O_3[a]	2.63	3.34	8.05	1.38	1.58	–	0.998, 0.979
1-$C_4H_8/Cr_2O_3/NO_2$	0.937	5.08	13.4	0.540	0.618	0.556	0.998, 0.995
C_2H_2/ZnO[a]	6.90	5.43	9.36	3.74	2.91	–	0.998, 0.993
C_2H_2/ZnO/NO_2	2.60	2.78	24.0	6.59	5.14	0.525	0.994, 0.992
C_2H_6/ZnO[a]	7.80	12.4	6.95	1.37	1.14	–	0.985, 0.981
C_2H_6/ZnO/NO_2	41.5	14.5	3.64	3.29	2.76	24.3	0.993, 0.963

The goodness of curve fitting is given by the squared correlation coefficient for both, the four exponential and the three exponential functions (r_4^2, r_3^2).

[a] Obtained from Ref. [10].

$$V_d = \frac{k_1 V'_G(\text{empty})\epsilon}{A_s} \cdot \frac{k_2}{k_{-1} + k_2} \quad (40)$$

where $V'_G(\text{empty})\epsilon$ is the gaseous volume (cm^3) of void space in the solid bed [cf. Eq. (29)] and A_s the total surface area (cm^2) of the solid. The V_d differs from the overall mass transfer coefficient to the solid surface K_G [4] only in the correction factor $k_2/(k_{-1}+k_2)$.

The reaction probability γ of the pollutant with the surface of the solid is found as before [8]:

$$\frac{1}{\gamma} = \left(\frac{R_g T}{2\pi M_B}\right)^{1/2} \cdot \frac{1}{V_d} + \frac{1}{2} \quad (41)$$

R_g being the ideal gas constant, T the absolute temperature and M_B the molar mass of the analyte.

From k_1, the isotherm is calculated as already reported [2].

All calculations described above are carried out in the same personal computer (PC) program in GW-BASIC given in the Appendix and used to calculate the B values. The H, t experimental pairs are entered in the DATA LINES 2000–2050, while the other known quantities [temperature T, lengths L_1 and L_2, gaseous volumes V_G and V'_G, external porosity of the solid bed ϵ, cross sectional area a_y, amount of adsorbent per unit length of bed a_s, specific surface area of solid SSA, molar mass of the analyte A M_B, and $\alpha_2(1+V_1)$] are entered in the INPUT LINES 200–300. Then, all parameters B_1, B_2, B_3, B_4, B_5, B_6, B_7, k_1, k_{-1}, k_2, k_{app}, V_d, γ and α_1 are printed in the given units. If one wants the adsorption isotherm explicitly printed, this can be done by means of the PC program already published [2].

The number of significant figures in Tables 1 and 2 is based on the standard errors of B values. It is difficult to estimate the final errors of k_1, k_{-1}, k_2, V_d, γ and k_{app}, since they come out as a result of the above complex series of calculations, and the application of the rule of error propagation in a long sequence of steps does not give reliable final errors.

3. Experimental

3.1. Materials

The $(CH_3)_2S$ used as pollutant analyte was a product of Fluka (puriss.), C_3H_6 was purchased from Linde (Athens, Greece), while the other hydrocarbons C_2H_2, C_2H_4, C_2H_6 and 1-C_4H_8 were obtained from Air Liquide (Athens, Greece) and had a purity of 99.000–99.999%.

The NO_2 was either purchased from Air Liquide or prepared in laboratory scale by heating $Pb(NO_3)_2$

Table 2
Local adsorption parameters (k_1), desorption rate constants (k_{-1}), surface reaction rate constants (k_2), deposition velocities (V_d), reaction probabilities (γ) and apparent gaseous reaction rate constants (k_{app}) of $(CH_3)_2S$ ($7.9 \cdot 10^{-3}$ mol/dm^3), interacting with particles of $CaCO_3$ (Penteli marble) and particles from the Statues Λ.1, Λ.87 and Λ.292, exhibits of the National Archaeological Museum in Kavala (Greece)

Solid	T (K)	C_{NO_2} (10^{-3} mol/dm^3)	k_1 (10^{-3} s^{-1})	k_{-1} (10^{-3} s^{-1})	k_2 (10^{-4} s^{-1})	V_d (10^{-9} cm s^{-1})	γ (10^{-12})	k_{app} (10^{-4} s^{-1})	r_4^2, r_3^2
$CaCO_3$	302.2	0.00	1.09	3.72	5.40	8.30	1.03	-	0.998, 0.999
$CaCO_3$	304.2	18.00	6.51	10.7	72.0	158	19.6	23.2	0.999, 0.999
$CaCO_3$	300.2	36.00	3.50	2.32	55.1	148	18.5	8.62	0.999, 0.998
$CaCO_3$	323.2	0.00	2.77	3.44	0.542	2.58	0.311	-	0.996, 0.995
$CaCO_3$	323.2	18.00	3.42	3.35	2.04	11.81	1.42	9.67	0.993, 0.992
$CaCO_3$	323.2	36.00	3.14	6.18	43.0	77.4	9.33	3.69	0.993, 0.991
Statue Λ.1	304.2	0.00	0.509	5.76	8.72	4.94	0.614	-	0.999, 0.999
Statue Λ.1	305.2	18.00	5.30	2.00	0.148	2.92	0.362	13.5	0.971, 0.959
Statue Λ.1	304.2	36.00	0.0074	39.0	445	4.45	0.553	30.3	0.952, 0.916
Statue Λ.1	323.2	0.00	0.587	9.72	15.9	6.09	0.733	-	0.992, 0.992
Statue Λ.1	323.2	18.00	21.8	0.175	8.69	1338	161	9.98	0.935, 0.934
Statue Λ.1	323.2	36.00	28.4	0.827	2.16	741	89.3	59.2	0.993, 0.981
Statue Λ.87	304.2	0.00	17.1	0.178	3.43	676	84.0	-	0.999, 0.999
Statue Λ.87	302.2	18.00	2.45	12.3	2.49	3.0	0.379	20.5	0.996, 0.996
Statue Λ.87	303.2	36.00	71.1	0.021	23.4	4792	596	6.05	0.996, 0.995
Statue Λ.87	323.2	0.00	77.4	0.0020	23.3	47 713	5751	-	0.999, 0.999
Statue Λ.87	323.2	18.00	70.3	0.280	2.33	1963	237	52.0	0.994, 0.992
Statue Λ.87	323.2	36.00	40.7	0.196	0.048	59.4	7.15	10.4	0.946, 0.945
Statue Λ.292	301.2	18.00	1.21	11.2	22.4	12.9	1.61	12.6	0.998, 0.995
Statue Λ.292	301.2	36.00	2.09	1.37	6.71	43.5	5.43	40.0	0.992, 0.990
Statue Λ.292	323.2	0.00	3.35	0.352	6.78	140	16.9	-	0.999, 0.999
Statue Λ.292	323.2	18.00	5.81	26.5	1.73	2.42	0.292	26.7	0.994, 0.989
Statue Λ.292	323.2	36.00	4.23	17.9	17.0	23.3	2.81	5.09	0.992, 0.988

The measurements were conducted in the absence and in the presence of NO_2, at two temperatures. The goodness of curve fitting is given by the squared correlation coefficient for both, the four exponential and the three exponential functions (r_4^2, r_3^2).

of analytical grade at atmospheric pressure, and collected under cooling with liquid nitrogen, in the absence of moisture.

The solids Cr_2O_3 and ZnO were pro-analysi products of Merck.

The marble was obtained from Penteli (Greece) and its analysis has been given before [9]. The solid samples from statues Λ.1, Λ.87 and Λ.292 were kindly offered by the National Archaeological Museum of Kavala, Greece.

The carrier gas was nitrogen (99.99%) from Linde, dried by silica gel or 13X molecular sieve, with a flow-rate of about 20 cm^3/min.

3.2. Apparatus

The experimental set-up is analogous to that outlined in Fig. 1 of Ref. [3], with some minor differences indicated in Fig. 1 of this paper. Section L_1 (21.7–51.6 cm) was empty of any solid material, while L_2 (2.9–7 cm) contained the solid bed. Both L_1 and L_2 were composed of pyrex glass with an I.D. of 3.5–24 mm and heated to the same temperature. The sampling column $l'+l$ (40+40 to 65+65 cm) was a stainless-steel chromatographic tube of 4 mm I.D. No separation column was used.

The chromatographs were Shimadzu 8A and 14, equipped with F.I.D. and F.P.D. detectors.

3.3. Procedure

After conditioning of the solid bed by heating it in situ at 473 K for 24 h, under a continuous carrier gas flow, the bed was cooled to the working temperature for 1 h. Then, the pollutant analytes were introduced through either of the injectors of Fig. 1 as gases (0.5–1 cm^3 at atmospheric pressure) or as liquids (2–8 μl), the latter being used for NO_2 and $(CH_3)_2S$. The second analyte NO_2 was injected 35 s after the first.

Following the appearance of the continuously rising concentration–time curve in the detector signal, the reversing procedure for the carrier gas flow was started, lasting 10–30 s for each reversal, which is shorter than the gas hold-up time in both column sections l' and l. The narrow fairly symmetrical sample peaks created by the flow reversals were recorded and their height H or the area under the curve was calculated and printed, together with the corresponding time t, by a C-R6A Shimadzu Chromatopac. By entering the pair values of H, t into the 2000–2050 DATA lines of the GW-BASIC program given in the Appendix, together with the other known quantities in the INPUT lines 200–300, all physicochemical parameters exposed and defined in Section 2 are calculated and printed.

4. Results and discussion

The main objective of the present paper is to present a new methodology rather than enriching databases with numerical results. Therefore, the results collected in this section are only to exemplify the method. This can be done by applying the methodology described in Section 2.3 to some systems pertaining to the action of air pollutants on metal oxides, on natural Penteli marble and on objects of cultural heritage inside an archaeological museum. The results listed in Tables 1 and 2 were obtained. For comparison purposes, the physicochemical parameters for the interaction of a gaseous pollutant A(g) with a solid surface S are given both, in the absence and in the presence of a second gaseous pollutant B(g), which was NO_2 in the present work. Section 2 describes the mathematical model and the calculations referring to the system A(g)+B(g)+S, but the relations derived are easily reduced to the system A(g)+S, by simply setting $k_{app}=0$. The numerical calculations leading to the results in Tables 1 and 2 for A(g)+S, were carried out by running a PC program in GW-BASIC given as Appendix in Ref. [10], similar to that given in the Appendix in this paper.

The air pollutants were chosen as examples of volatile hydrocarbons due mainly to anthropogenic emissions, and dimethyl sulfide (emitted by oceanic phytoplankton) as the major natural source of sulfur in the troposphere.

Regarding nitrogen dioxide used as a second pollutant, it is well known that this is very abundant in the atmosphere.

A comparison of the results in Tables 1 and 2 shows that in most cases all physicochemical parameters change in the presence of NO_2. At the same temperature, the deposition parameters of hydrocarbons on Cr_2O_3 and ZnO in some cases remain unaffected by the presence of NO_2 (cf. C_2H_2/Cr_2O_3 and $C_2H_2/Cr_2O_3/NO_2$), while in other cases suffer a detectable change. These changes are usually bigger in the experiments with dimethyl sulfide and Penteli marble or particles from the museum statues. The presence of synergistic effects in hydrocarbons/ NO_2 or dimethyl sulfide/NO_2 is fairly obvious, although the direction and magnitude of the changes is difficult to explain. Naturally, one thinks of the detailed mechanism of the phenomena which is so far unknown, and which almost certainly include blocking of adsorption active sites by NO_2 molecules or creation of new ones by it.

Acknowledgments

The financial support of the European Commission (DG-XII, contract EV 5V-CT94-0537) is gratefully acknowledged. Also, the authors wish to thank the National Archaeological Museum in Kavala (Greece) for their kind collaboration and the Ministry of Civilization for granting permission to obtain samples from the exhibited statues. Finally, thanks are due to Miss Anna Malliori for the typescript preparation.

Appendix 1

```
10 REM Non-Linear Regression Analysis of Function:
20 REM H^(1/M)=A1*EXP(B1*T)+S*A2*EXP(B2*T)+P*A3*EXP(B3*T)+X*A4*EXP(B4*T)
30 REM H^(1/M)=A5*EXP(B5*T)+S*A6*EXP(B6*T)+P*A7*EXP(B7)
40 REM Calculation of kinetic parameters with non-linear isotherms and
       experimental set-up of Chromatographia 41(1995)227,with injection
       of one or two gaseous substances, at y=0 or y=L2.
50 REM     N2    = Minimum number of points of first exponential function
60 REM     MAX   = Square of maximum correlation coefficient
70 REM     OPT   = Final optional choice of variables when OPT=1
80 REM     J     = Number of points of first exponential function
90 REM     G     = Number of points of second exponential function
100 REM     F     = Number of points of third exponential function
110 REM    K,L   = First and last point of linear regression in subroutine
120 REM    SA,SB = Standard errors of A and B in each linear regression
130 REM    Y(I)  = Ordinate for each linear regression in the subroutine
140 REM    U(I)  = Variable remaining by  removal of the previous one, two or
                   three exponential functions
150 REM    D(I)  = Function for calculating the correlation coefficient
160 INPUT "Total number of pairs H,T=";N
170 DIM H(N),T(N),Y(N),U(N),D(N)
180 INPUT "Response factor=";M
190 INPUT "Factor to divide H(I)=";H1
200 INPUT "Temperature in K=";T
210 INPUT "Lenth L1(cm) of Section z=";L1
220 INPUT "Length L2(cm) of Section y=";L2
230 INPUT "Gaseous Volume VG1(cm^3) of Empty Section L1=";VG1
240 INPUT "Gaseous Volume VG2(cm^3) of Empty Section L2=";VG2
250 INPUT "External Porosity of the Solid bed,E=";E
260 INPUT "Cross Sectional Area AY(cm^2) of Void Space in Region y=";AY
270 INPUT "Amount of Adsorbent per Unit Length of Bed AS(g/cm)=";AS
280 INPUT "Specific Surface Area of Solid SSA(cm^2/g)=";SSA
290 INPUT "Molar Mass MB(kg/mol) of Analyte B=";MB
300 INPUT "a2(1+V1) Calculated by Program of Appendix A of ref.(10)=";AV
310 FOR I=1 TO N
320    READ H(I),T(I)
330    H(I)=H(I)/H1
340 NEXT I
350 N2=INT(N/7+.5)
360 MAX=0:OPT=0
370 REM Calculation of A1 and B1 with H,T pairs ranging from N2 to N-2*N2-3
380 FOR J=N2 TO N-2*N2-3
390    K=N-J+1
400    L=N
410    FOR I=K TO L
420       Y(I)=(1/M)*LOG(H(I))
430    NEXT I
440    GOSUB 2400       :REM Subroutine for linear regression analysis
450    A1=EXP(A)
460    B1=B
470    SA1=SA
480    SB1=SB
490    IF OPT=1 THEN  530
500 REM Calculation of A2 and B2 with H,T pairs ranging from N2 to N-J-N2-3
        ,and both prefixes -1 or +1
510    FOR S=-1 TO +1 STEP 2
520       FOR G=N2 TO N-J-N2-3
530          K=N-J-G+1
```

```
540            L=N-J
550           FOR I=K TO L
560              U(I)=S*H(I)^(1/M)-S*A1*EXP(B1*T(I))
570              Y(I)=LOG(ABS(U(I)))
580           NEXT I
590           GOSUB 2400    :REM Subroutine for linear regression analysis
600           A2=EXP(A)
610           B2=B
620           SA2=SA
630           SB2=SB
640           IF OPT=1 THEN 680
650 REM Calculation of A3 and B3 with H,T pairs ranging from N2 to N-J-G-3
       and both prefixes -1 or +1
660           FOR P=-1 TO +1 STEP 2
670              FOR F=N2 TO N-J-G-3
680                 K=N-J-G-F+1
690                  L=N-J-G
700                 FOR I=K TO L
710                    U(I)=P*(H(I)^(1/M)-A1*EXP(B1*T(I))-S*A2*EXP(B2*T(I)))
720                    Y(I)=LOG(ABS(U(I)))
730                 NEXT I
740                 GOSUB 2400    :REM Subroutine for linear regression analysis
750                 A3=EXP(A)
760                 B3=B
770                 SA3=SA
780                 SB3=SB
790                 IF OPT=1 THEN 820
800 REM Calculation of A4 and B4 with H,T pairs ranging from 1 to N-J-G-F,and
       both prefixes -1 or +1
810                 FOR X=-1 TO +1 STEP 2
820                    K=1
830                    L=N-J-G-F
840                    FOR I=K TO L
850                       U(I)=X*(H(I)^(1/M)-A1*EXP(B1*T(I))-S*A2*EXP(B2*T(I))-P*
                                A3*EXP(B3*T(I)))
860                       Y(I)=LOG(ABS(U(I)))
870                    NEXT I
880                    GOSUB 2400  :REM Subroutine for linear regression analysis
890                    A4=EXP(A)
900                    B4=B
910                    SA4=SA
920                    SB4=SB
930                    IF OPT=1 THEN 1130
940                    C1=0
950                    C2=0
960                    C3=0
970                    FOR I=1 TO N
980                       D(I)=H(I)^(1/M)-A1*EXP(B1*T(I))-S*A2*EXP(B2*T(I))-P*A3*
                                EXP(B3*T(I))-X*A4*EXP(B4*T(I))
990                       C1=C1+D(I)^2
1000                       C2=C2+H(I)^(2/M)
1010                       C3=C3+H(I)^(1/M)
1020                    NEXT I
1030                    R=1-C1/(C2-C3^2/N)
1040                    IF R>MAX THEN MAX=R:SMAX=S:PMAX=P:XMAX=X:JMAX=J:GMAX=G:
                          FMAX=F
1050                 NEXT X
1060              NEXT F
1070           NEXT P
1080        NEXT G
1090     NEXT S
1100 NEXT J
1110 S=SMAX:P=PMAX:X=XMAX:J=JMAX:G=GMAX:F=FMAX:OPT=1
1120 GOTO 390
1130 LPRINT "Intercept Ln(A1) and its Standard error =";LOG(A1*H1) "+-"SA1
1140 LPRINT "Slope B1 and its Standard error=";B1 "+-"SB1
1150 LPRINT
1160 LPRINT "Intercept Ln(A2) and its Standard error=";LOG(A2*H1) "+-"SA2
1170 LPRINT "Slope B2 and its Standard error=";B2 "+-"SB2
1180 LPRINT
1190 LPRINT "Intercept Ln(A3) and its Standard error=";LOG(A3*H1) "+-"SA3
1200 LPRINT "Slope B3 and its Standard error=";B3 "+-"SB3
1210 LPRINT
1220 LPRINT "Intercept Ln(A4) and its Standard error=";LOG(A4*H1) "+-"SA4
1230 LPRINT "Slope B4 and its Standard error=";B4 "+-"SB4
```

```
1240 LPRINT
1250 LPRINT "Square of maximum correlation coefficient r^2=";MAX
1260 LPRINT "Optimum values of points for 1st, 2nd , 3rd and 4th exponential
            functions, respectively=";JMAX","GMAX","FMAX"and"N-JMAX-GMAX-FMAX
1270 LPRINT "Values of S,P and X,respectively ="; SMAX","PMAX"and"XMAX
1280 LPRINT
1290 N2=INT(N/6+.5)
1300 MAX=0:OPT=0
1310  REM Calculation of A5 and B5 with H,T pairs ranging from N2 to N-N2-3
1320 FOR J=N2 TO N-N2-3
1330    K=N-J+1
1340    L=N
1350    FOR I=K TO L
1360       Y(I)=(1/M)*LOG(H(I))
1370    NEXT I
1380    GOSUB 2400         : REM Subroutine for linear regression analysis
1390    A5=EXP(A)
1400    B5=B
1410    SA5=SA
1420    SB5=SB
1430    IF OPT=1 THEN  1470
1440  REM Calculation of A6 and B6 with H,T pairs ranging from N2 to N-J-3 and
      both prefixes -1 and +1
1450    FOR S=-1 TO +1  STEP 2
1460       FOR G=N2 TO N-J-3
1470          K=N-J-G+1
1480          L=N-J
1490          FOR I=K TO L
1500             U(I)=S*H(I)^(1/M)-S*A5*EXP(B5*T(I))
1510             Y(I)=LOG(ABS(U(I)))
1520          NEXT I
1530          GOSUB 2400     : REM Subroutine for linear regression analysis
1540          A6=EXP(A)
1550          B6=B
1560          SA6=SA
1570          SB6=SB
1580          IF OPT=1 THEN 1610
1590  REM Calculation of A7 and B7 with H,T pairs ranging from 1 to N-J-G,
      with both prefixes -1 and +1
1600          FOR P=-1 TO +1 STEP 2
1610             K=1
1620             L=N-J-G
1630             FOR I=K TO L
1640                U(I)=P*(H(I)^(1/M)-A5*EXP(B5*T(I))-S*A6*EXP(B6*T(I)))
1650                Y(I)=LOG(ABS(U(I)))
1660             NEXT I
1670             GOSUB 2400    : REM Subroutine for linear regression analysis
1680             A7=EXP(A)
1690             B7=B
1700             SA7=SA
1710             SB7=SB
1720             IF OPT=1 THEN 1900
1730             C1=0
1740             C2=0
1750             C3=0
1760             FOR I=1 TO N
1770                D(I)=H(I)^(1/M)-A5*EXP(B5*T(I))-S*A6*EXP(B6*T(I))
                         -P*A7*EXP(B7*T(I))
1780                C1=C1+D(I)^2
1790                C2=C2+H(I)^(2/M)
1800                C3=C3+H(I)^(1/M)
1810             NEXT I
1820             R=1-C1/(C2-C3^2/N)
1830             IF R>MAX THEN MAX=R:SMAX=S:PMAX=P:JMAX=J:GMAX=G
1840          NEXT P
1850       NEXT G
1860    NEXT S
1870 NEXT J
1880 S=SMAX:P=PMAX:J=JMAX:G=GMAX:OPT=1
1890 GOTO 1330
1900 LPRINT "Intercept Ln(A5) and its Standard error=";LOG(A5*H1) "+-"SA5
1910 LPRINT "Slope B5 and its Standard error=";B5 "+-"SB5
1920 LPRINT "Intercept Ln(A6) and its Standard error=";LOG(A6*H1) "+-"SA6
1930 LPRINT "Slope B6 and its Standard error=";B6 "+-"SB6
```

```
1940 LPRINT "Intercept Ln(A7) and its Standard error=";LOG(A7*H1) "+-"SA7
1950 LPRINT "Slope B7 and its Standard error=";B7 "+-"SB7
1960 LPRINT
1970 LPRINT "Square of maximum correlation coefficient r^2=";MAX
1980 LPRINT "Optimum values of points for 1st, 2nd and 3rd exponential
            functions,respectively=";JMAX","GMAX"and"N-JMAX-GMAX
1990 LPRINT "Values of S and P, respectively =";SMAX"and"PMAX
2000 DATA
2010 DATA
2020 DATA
2030 DATA
2040 DATA
2050 DATA
2060 X=-(B1+B2+B3+B4)/60
2070 Y=(B1*B2+B1*B3+B1*B4+B2*B3+B2*B4+B3*B4)/60^2
2080 Z=-(B1*B2*B3+B1*B2*B4+B1*B3*B4+B2*B3*B4)/60^3
2090 W=(B1*B2*B3*B4)/60^4
2100 X1=-(B5+B6+B7)/60
2110 Y1=(B5*B6+B5*B7+B6*B7)/60^2
2120 Z1=-(B5*B6*B7)/60^3
2130 V1=2*VG2*E/VG1+(L2^2/L1^2)
2140 SK(1)=X-X1:SK(2)=W/Z1:SK(3)=(SK(1)+SK(2))/2:            REM SK=k_1+k2
2150  FOR I=1 TO 3
2160 AVKAPP=X-SK(I)
2170 A2V1=AV*V1/(1+V1)
2180 A2=AV/(1+V1)
2190 KAPP=(AVKAPP-AV)/2
2200 K1K3=(Y-AVKAPP*SK(I)-Z/SK(I)+W/(A2V1+KAPP)/SK(I))/(1-(A2V1+KAPP)/SK(I))
2210 K1K3=ABS(K1K3)
2220 K2=W/(A2V1+KAPP)/K1K3
2230 K3=SK(I)-K2 :K3=ABS(K3)
2240 K1=K1K3/K3
2250 A11 =(Y-AVKAPP*SK(I)-K1K3-KAPP^2-AV*KAPP)/A2
2260  A12=(Z-A2V1*K1K3-K1K3*K2-AV*KAPP*SK(I)-K1K3*KAPP-KAPP^2*SK(I))/SK(I)/A2
2270  VD=K1*VG2*E*K2/(SSA*AS*L2*SK(I))
2280  G1=SQR(1.32321*T/MB)/VD*100+.5
2290  G2=1/G1
2300  LPRINT "k1 in 1/s=";K1
2310  LPRINT "k_1 in 1/s=";K3
2320  LPRINT "k2 in 1/s=";K2
2330  LPRINT "Deposition velocity in cm/s=";VD
2340  LPRINT "Reaction probability =";G2
2350  LPRINT "kapp in 1/s=";KAPP
2360  LPRINT "a1 in 1/s=";A11;","A12
2370  LPRINT
2380 NEXT I
2390 END
2400  REM Linear regression of Y(I) = A + B T(I)
2410 S1=0
2420 S2=0
2430 S3=0
2440 S4=0
2450 S5=0
2460    FOR I=K TO L
2470    S1=S1+T(I)
2480    S2=S2+T(I)^2
2490    S3=S3+Y(I)
2500    S4=S4+Y(I)^2
2510    S5=S5+T(I)*Y(I)
2520 NEXT I
2530 Z=L-K+1  :REM Number of points for the linear regression analysis
2540 M1=S5-S1*S3/Z
2550 M2=S2-S1^2/Z
2560 M3=S4-S3^2/Z
2570 A=(S3-S1*M1/M2)/Z
2580 B=M1/M2
2590 SYT=SQR(ABS(S4-A*S3-B*S5)/(Z-2))
2600 SA=SYT*SQR(S2/Z/M2)
2610 SB=SYT/SQR(M2)
2620 RETURN
```

References

[1] N.A. Katsanos, F. Roubani-Kalantzopoulou, J. Chromatogr. A 710 (1995) 191–228.

[2] V. Sotiropoulou, G.P. Vassilev, N.A. Katsanos, H. Metaxa, F. Roubani-Kalantzopoulou, J. Chem. Soc. Faraday Trans. 91 (1995) 485–492.

[3] I. Topalova, A. Niotis, N.A. Katsanos, V. Sotiropoulou, Chromatographia 41 (1995) 227–235.

[4] N.A. Katsanos, Ch. Vassilakos, J. Chromatogr. 557 (1991) 469–479.

[5] A. Niotis, N.A. Katsanos, Chromatographia 34 (1992) 398–410.

[6] J. Kapolos, N.A. Katsanos, A. Niotis, Chromatographia 27 (1989) 333–339.

[7] N.A. Katsanos, Flow Perturbation Gas Chromatography, Marcel Dekker, New York, Basel, 1988, p. 119.

[8] E. Arvanitopoulou, N.A. Katsanos, H. Metaxa, F. Roubani-Kalantzopoulou, Atmos. Environ. 28 (1994) 2407–2412.

[9] N.A. Katsanos, G. Karaiskakis, J. Chromatogr. 395 (1987) 423–435.

[10] F. Roubani-Kalantzopoulou, A. Kalantzopoulos and N.A. Katsanos, in preparation.

[11] A.J. Sedman, J.G. Wagner, J. Pharm. Sci. 65 (1976) 1006–1010.